A Markov-based Framework For Handover Process in Heterogenous Networks

By

Saba Farooq Balouch

FALL-2015-MSSYSE00000118123

Supervisor

Dr. Mian Ilyas Ahmad

Department of Computational Engineering

A thesis submitted in partial fulfillment of the requirements for the degree of Masters of Science in Computational Science and Engineering (MS CS&E)

In

Research Center for Modeling and Simulation,

National University of Sciences and Technology (NUST),
Islamabad, Pakistan.
(November 2018)

Approval

It is certified that the contents and form of the thesis entitled " **A Markov-based Framework For Handover Process in Heterogenous Networkss**" submitted by **Saba Farooq Balouch** have been found satisfactory for the requirement of the degree.

Advisor: **Dr. Mian Ilyas Ahmad**

Signature: _____

Date: _____

Committee Member 1: **Dr. Shahzad Rasool**

Signature: _____

Date: _____

Committee Member 2: **Dr. Salman Ghafoor**

Signature: _____

Date: _____

Dedicated to my parents for their love, endless support and encouragement

Certificate of Originality

I hereby declare that this submission is my own work and to the best of my knowledge it contains no materials previously published or written by another person, nor material which to a substantial extent has been accepted for the award of any degree or diploma at NUST RCMS or at any other educational institute, except where due acknowledgement has been made in the thesis. Any contribution made to the research by others, with whom I have worked at NUST RCMS or elsewhere, is explicitly acknowledged in the thesis. I also declare that the intellectual content of this thesis is the product of my own work, except for the assistance from others in the project's design and conception or in style, presentation and linguistics which has been acknowledged.

Author Name: **Saba Farooq Balouch**

Signature: _____

Acknowledgement

I would not be able to complete the work that is presented in this thesis without help of many people who were around me during my M.S. studies. I would like to express my deepest gratitude to my advisor and mentor, Dr. Mian Ilyas Ahmad, for providing me this wonderful and career-changing opportunity to work under his guidance for my M.S. I am profoundly thankful to his boundless energy and encouragement to help me steadily progress in my research direction. I am also thankful for his guidance and mentoring towards shaping my career path.

I would also like to extend my appreciation to Dr. Shahzad Rasool for helping me throughout my thesis and for always discuss various challenges in my studies. His intriguing questions have been inspiring and have helped me to improve my work.

Besides my advisor, Dr. Salman Abdul Ghafoor efforts are also noteworthy to have imparted his insightful comments and encouragement during the journey of the thesis. It not only provoked me to widen my research but also their support in learning was admirable.

Apart from the research team, I would like to thank my close friends exclusively Ahamd Shahan, Hadia Afzaal and Aroosh Fatima whose kind support has always ensured my true potential. Last but not the least, my gratitude goes to my family:my parents for continuous encouragement, prayers and unshakable believe. Their spiritual and moral support throughout the thesis phase will truly be remembered in my life.

Saba Farooq Balouch

List of Abbreviations

CDN	Content Distribution Network
CAHP	Context-aware handover policy
f_c	Carrier Frequency
HetNets	Heterogeneous Network
LTE	Long Term Evolution
QOS	Quality of Service
RLF	Radio Link Failure
RSS	Received Signal Strength
SON	Self-organizing networks
T_c	Coherence time
TCP	Transmission Control Protocol
T_H	Threshold
TTT	Time to Trigger
UE	User Equipment
WLAN	Wireless Local Area Network
SINR	Signal to interference plus noise ratio
HOR	Handover Rate
HM	Hysteresis Margin
CRE	Cell Range Expansion

Contents

List of Tables

List of Figures

Abstract

Due to the increase in demand of high data traffic, mobile networks are evolving from single overlay network to a complex mixture of network technologies referred as Heterogeneous networks (HetNets). Such networks require smooth transition of communication link when user moves from one cell to another cell region of HetNets, called handover (HO). There are several issues in handover process. Our aim is to analyze handover scenarios, key parameters of HO, success and failure of HO rate (HOR) which affects the performance. HO occurs when signal to noise ratio is less than predefined threshold. In this thesis we analyze the performance of handover under different parameters, such as received signal strength (RSS), hysteresis margin (HM) and Cell Range Expansion (CRE). A Markov based framework is used to model the handover process for the user equipment (UE) by defining different positions of the UE at a possible trajectory as the Markov states. With the change in UE, its SINR changes accordingly. This behavior is modelled in Markov chain by using transfer probabilities, where at a particular state the UE can stay in the same state or is in motion. A few transitions of the Markov chain from a given initial state can specify the HOR of the network. To analyze the effect of the above parameters on HOR, we consider a single macro cell and femto cell with a UE following a specific trajectory towards the femto cell. Distances of UE along the trajectory from both macro and femto cell are computed that are used to find distance dependent path losses. This allows us to compute received signal strength which in turn identifies the transfer probabilities of each state. Finally the performance of HOR is analyzed through transitions of the Markov chain. It is observed that there is a decrease in HOR as the values of CRE, HM and number of states increases. The main purpose of this work is to observe efficient handover criteria in heterogeneous cellular networks so that the overall quality of communication service improves.

Chapter 1

Introduction

1.1 Overview

The increasing demand of high data traffic is one of the principal challenges in wireless cellular network. In recent years, the rise of cell phones and tablets with bandwidth-exhaustive tasks for instance audio and video streaming, online gaming, social networking and cloud computing have led to an outburst in the demand for data traffic [1] in cellular networks.

To overcome this issue, mobile networks are evolving from single overlay network to a complex mixture of network technologies commonly referred as Heterogeneous networks (HetNets). The idea is to identify small networks in the cellular range of a large network and assign some data traffic to smaller networks without effecting the quality of service.The implementation of heterogeneous networks however require numerous technical trials to ensure proper service managements. Examples of some technical problems include cell selection and handover procedures that are crucial to provide reliable services when users move in or out of a particular cell coverage area.

The aim of this thesis is to mathematically analyze handover scenarios, key parameters of handover, success and failure of handover as well as frequency of handover.

1.2 Systems Engineering and HetNets

Systems engineering (SE) is an interdisciplinary field of engineering whose focus is on the analysis, design and development of complex technological systems. Moreover, in systems engineering analysis, multiple alternatives are observed so that the most suitable one can be selected. Heterogeneous network is a network which is composed of different type of cells. Each cell type can be considered as a subsystem. All these subsystems are integrated to increase the efficiency of communication in the fixed coverage area and achieve good signal strength with variations in different parameters. By doing so, we are not only dealing with subsystems but also with the impact of one subsystem on another subsystem and on the overall system.

An important aspect of systems engineering is to keep the customers need intact with desired functionality. Heterogeneous network for communication is an important complex system which directly affect customer's needs. Using systems engineering principles, it is important to analyze these HetNets and suggest possible improvements.

Figure 1.1 shows a typical HetNet where a macro base station (BS) is installed in an area that is responsible for elementary coverage and communication at high power levels (5W to 400W). Smaller cells such as pico and femto cells are used for providing high data-rate services to smaller areas with dense traffic. Femto cells can provide services to several devices surrounded by a range of few hundred meters and femtocells are generally used for indoor or home networks. Owing to their short range, femtocells are more power efficient. Table 1.1 shows different cell types along with their cell ranges and characteristics of the cell types.

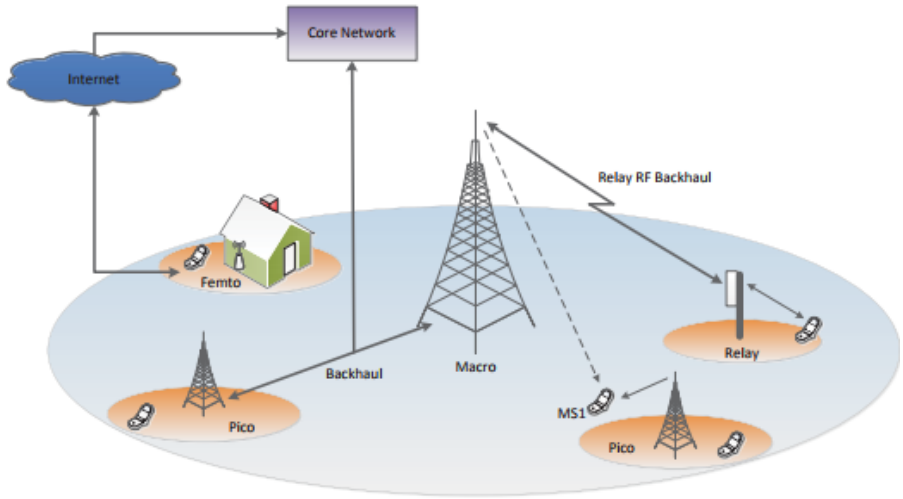

Figure 1.1: Heterogeneous Cellular Network

.

1.3 Handover (HO)

In wireless cellular communication, handover (HO) is stated as the switching from one set of radio resources to another set. Handover is a fundamental concept in scheduling and positioning of the cellular networks. It permits users to create data sessions or connect phone calls on the move. For example, if mobile user moves away from its serving base station, its signal starts to degrade which can results in poor signal reception and can also result in disconnection of services. However, before the decrease of signal strength below certain threshold, handover is performed so that an alternate reception with better signal strength is selected for communication, if available. There are several issues in handover process, such as unnecessary handover and handover failure, which effect the performance of communication. In this thesis we analyze the performance of handover.

The mathematical model is then used to design such policy that chooses the HO parameters to take full advantage.

Table 1.1: Comparison of Cell Types in HetNets

Characterstics	Femto	Pico	Micro	Macro
Indoor/Outdoor	Indoor	Indoor/Outdoor	Outdoor	Outdoor
Number of Users	4 to 16	32 to 100	200	200 to 1000+
Maximum output power	20 to 100mW	250mW	2 to 10W	40 to 100W
Maximum cell radius	10 to 50m	200m	2km	10 to 40km
Access Network	Closed	Open	Open	Open
Bandwidth	10MHz	20MHz	20 to 40MHz	60 to 75 MHz

1.4 Problem Statement

HO process is linked to the distance of the user from base station, path loss of the signal, received signal strength, cell range expansion and hysteresis margin or threshold. All these parameters have to be analyzed along the user path for accurate decision of handover. For this purpose Markov Chain can be used to model the discrete samples (states) of the user path. The analysis of HO through Markov chain and the effect of the above parameters on handover through modelling and simulation is the problem considered in this thesis. The analysis helps in HO management that include unnecessary HO, HO failures and HO frequency.

1.5 Motivation

Communication is crucial for modern world and the world is evolving towards global village. Heterogeneous network is a term used for mobile communication networks which involves the combination of different access technologies and diverse cell types. Heterogenous network deployment is one of the most effective solutions for mobile users with the aim of decreasing the blocking from macro base stations. It is an

effective way to offload the data traffic and transfer them to femto cells for getting high data rates. In HetNets, there come several issues in handover process. HO process is of main importance within any cellular network. It is essential to ensure it can be implemented reliably and without interruption to any cells. HO is one of the important performance indicators observed so that a strong cellular handover is sustained on the cellular network. Thus, it is important to come up with a solution that deals with the performance of handover under different parameters.

1.6 Objectives

The objectives of this thesis are listed below.

- Modelling of handover process through Markov Chain.
- Analysis of handover policies
- Impact of handover regulation on user performance capacity and transition probabilities.
- Analysis of handover in regard to variation of different context parameters i.e.

1. Signal Strength
2. Handover Rate
3. Hysteresis Margin
4. Cell Range Expansion

These objectives are shown in figure 1.2

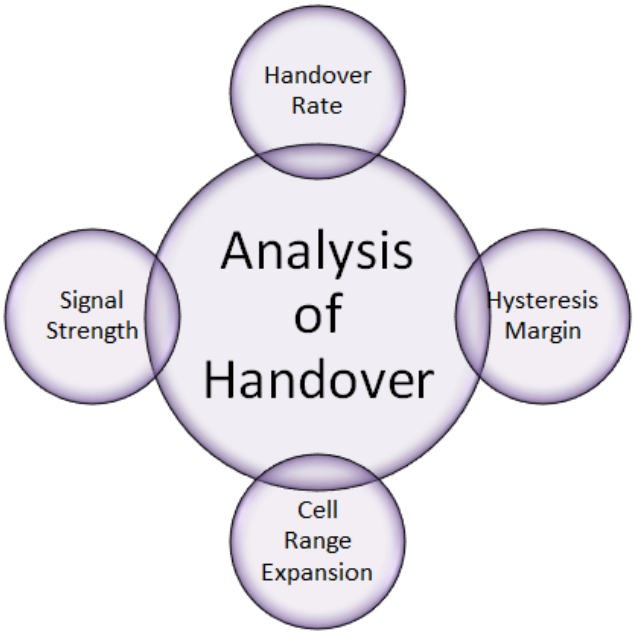

Figure 1.2: Thesis Contribution and Outcomes

.

1.7 Thesis Outlines

The remainder of the thesis is structured as follows:

In Chapter 2, literature survey on problem statement is presented. Chapter 3, methodology presents the model parameters of system for context aware HO which includes the analysis of several papers that were carried out in the field of handover and system design (Methodology) contains all the methods and steps in great details that were undertaken to achieve the project's objectives. Proposed model that is being used in this thesis and context parameters are illustrated along with a discussion. Chapter 4 shows results and discussions on simulation parameters obtained by experimenting on the proposed model. A discussion on the simulation and the resulted outcome are carried out. The thesis concludes in Chapter 5, the research contributions are summarized and future research directions are identified.

Chapter 2

Literature Review

In this chapter, existing approaches for handover and the associated research issues are discussed. Different researchers have proposed different methodologies to manage handover process in HetNets. This chapter discusses some of these techniques and presents possible analysis approach in a particular Markov based framework.

2.1 Handover in Heterogeneous Networks

Handover (HO) is the process by which mobile telephone calls are transferred from one base station to another as the user passes the boundary of its cell. In HetNets, there are multiple cells of different sizes and thus handover is more frequent. Some of the issues related to handover in HetNets are listed below.

- Unnecessary Handovers
- Handover Failure
- Handover frequency
- Handover variations (due to cell range expansion, RSS and hysteresis margin).

To address these issues, there are different contributions in the literature. Some of the well-known HO schemes are discussed in section below.

2.2 Different Approaches for HO

Handover process is controlled by handover schemes that are effectively improving the capacity and quality of service of cellular systems. HO schemes can be classified horizontally and vertically. Vertical handover schemes are established on the perception of scheme implement, while in case of horizontal it depends on identification of new BS that is built on received signals or prediction techniques.

On the basis of approaches and decision criteria of HO, vertical handover schemes are discussed in the following. Decisions of handover can be static or dynamic. Few key parameters to consider are coverage area of network, bandwidth, quality of link which includes received signal strength (RSS), signal to interference and noise ratio (SINR), reference signal received power (RSRP). RSS, which is a dynamic criteria of handover based algorithm relate RSS of current point of connection compared to the rest of the other to make HO decisions.

A large number of studies have been done in RSS based handover algorithms. [9], [16], [18], [21], [22], [23]. The conditions of HO decision in these references include:

- if RSS new $>$ RSS old then choose the new BS.
- if RSS new $>$ RSS old and RSS old $< T_h$.

We choose new BS having high RSS as compared to the BS with low RSS and the lower level is decided by threshold T_h. In terms of Hysteresis Margin, the condition of handover decision can be written as,

- if RSSnew $>$ RSSold + H

We may choose the new base station (BS) which has RSS with hysteresis margin H. There are various algorithms which are based on RSS for vertical handover decisions. Researchers suggested an algorithm for WLAN [13] & 3G networks based on RSS

in mixture with an expected lifetime to decide the time of HO. Its advantage is that it offers variations to user mobility & application requirements. Variations in available bandwidth is also a plus point of using this algorithm. Shortcomings includes delay in packets which causes rise in the lifespan of connectivity which is due to the weakening of channel conditions. Researchers recommended such an algorithm for wireless networks and WLAN which helps in the calculation of dynamic threshold [28] and then to compare it with the projected traveling time to help with decisions in handovers inside the WLAN.

a bandwidth based VHD algorithm between WLAN and WCDMA networks have been proposed in [12], [16], [14] that uses SINR as its key standard. This algorithm creates balance between WLAN and WCDMA network. This methodology presents excessive HO of SINR and possibly will results in a ping pong rate between access points.

Issues can be solved by using different parameters to control handover rate (HOR). On the whole, 3rd Generation Partnership Project 3GPP [19], is initiated by the User Equipment (UE), which at times measures the Reference Signal Receive Power (RSRP) from the surrounding cells. While the difference between the RSRP of an adjacent cell and that of the serving cell is greater than a fixed hysteresis value [24], the HO process initiates.

By means of large values of hysteresis margin and TTT, UE will possibly parctice a lower quality of RSRP during TTT phase as soon as it crosses a small cell, an issue that is in general stated to as handover (HO) Failure. Conversely, low hysteresis margin and short TTT may possibly cause HO Ping-Pong which is stated as the occurrence of numerous handovers to and from M-BS that produces loss in performance due to HO times and signaling overhead. To reduce handover failure and ping-pong rates these two contradictory objectives and HO plan needs to exchange

the two aspects [30]. Connection between handover failures and ping-pong rates as an element of TTT, hysteresis margin and user speed is presented in [26]. Authors of this paper demonstrate, UE can distinguish in its mobility form by observing the deviations of the type of HO failure events and in consequence to all this it can regulate the quantified Cell Individual Offset (CIO) parameter to reduce both the ping-pong rates and HO failure.

Researchers suggested in [33], where the researchers established a mathematical model for the handover process and develop an outage probability of user equipment (UE). Their strategy chooses the TTT and borderline parameters with the aim of universal model, and describes a HO policy based on more accurate statement that UEs trajectory with respect to location of the BSs is unknown.

A study of universal user trajectories are presented in [33] which authors researchers endorse accurate user mobility model, and present competent terminologies for the HO rate which is the estimated number of HOs per unit time and the cell sojourn time which is the estimated time in which a user stays inside a specific allocated cell.

Wide-ranging simulation movement is showed in self-organizing networks (SONs) [35] to compute the Radio Link Failure (RLF) in which researchers showed that usually RLF is acknowledged when (SINR) signal to noise ratio remains below a definite threshold for calculated aggregate of time that is usually 1s. RLF for diverse speeds and forms of handovers. The projected strategy picks the TTT parameter that promises that the RLF rate is lower than a certain threshold.

K. Kitagawa in [36] examined the Cell Range Expansion (CRE) procedure comprises in extending cell coverage with the purpose of stabilizing the users load. Researchers did simulation to evaluate the effect of CRE bias and HM on failure of handover and ping-pong rates, while setting the TTT parameter. Mobility prediction algo-

rithm [37] has been presented which is based on handover decision that evaluates the habitation time of the user equipment of the UE in the promising target cell. UE is allowed make variations in the target cell by projected policy only in that case when the predicted dwelling time is above a certain threshold. To reduce number of unnecessary handover in macro-femto cell networks, it's important to avoid macro to femto cell handovers of temporary HO visitors who stay in femto for comparatively short span of time. A smart HO decision algorithm is proposed for prevention of unnecessary HO's caused by temporary visitors.

2.3 Markov Chain for Handover Analysis

Markov chain is a well-known mathematical framework for modeling and analysis of different discrete processes. It has also been used in analyzing and managing handover processes in HetNets. Researchers[42] proposed that markov based framework can be used to combine handover algorithms with Call Admission Control policies in vehicular networks to increase efficiency for multiusers scenarios. Some authors have also proposed markov based framework for handover optimization [25].

Markov Chain process (MCP) was proposed to model user state during handover process and to find CRE[41], HM and TTT values. To overcome issues of load unbalancing, CRE, HM and TTT are applied in the system. By using MCP, we anlayze the effect of above mentioned parameters on handover that how these parameters effect the handover performance. How user directions are affecting signal strength and other parameters in all four quadrants. By using different angles at all quadrants, we are also able to compute how it affects its performance. In the end, we judge effect of its handover rate. Finally simulations are conducted to validate the effectiveness of the proposed method.

Chapter 3

Methodology

To analyze handover process, in this chapter,we discussed system model, distances for system model, the handover process, its performance model and state probabilities using Markov Chain.

3.1 Basic Framework for Handover Analysis

We utilized the concept of Markov chain to model the handover process into markov chain states. As a test case, we consider a single macro base station (M-BS) and a femto base station (F-BS) at a fixed distance from the two base stations (BS). We assume that a user equipment can follow multiple straight paths at different angles in entering the boundary of Femto cell from the Macro cell. A single path is shown in figure 3.2, where femto boundary is crossed at point b. The research methodology is classified as follows:

- Divide the complete path into some sample points and find distances of these points from macro and femto cells by using trigonometric functions.
- After computing distances from their respective base stations, we need to find distance dependent path losses for M-BS as well as for F-BS.

- Received signal strength (RSS) at each sample point can be computed.
- The values of received signal strength from the macro and femto cells together with cell range expansion and hysteresis margin define state transition probabilities where each sample point is considered as a state of markov chain (MC).
- Identify state transition matrix for markov chain and starting from an initial state we can identify the transitions of the state by using.

$$V_x = V_i \prod_{i=1}^{x} T(i) \tag{3.1}$$

where,

V_x = State probability vector at x-th step.

V_i = Probability of UE$'$s initial state.

T(i) = Markov Transfer Matrix.

- After knowing state vector at each transition, state transition vector also tells us about handover (HO) to occur.

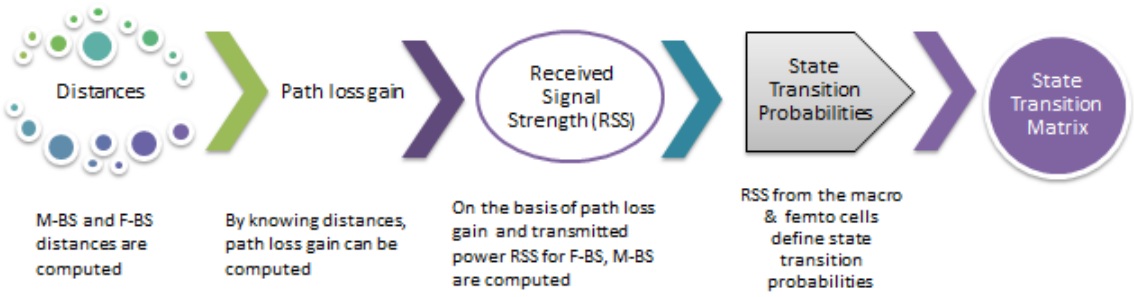

Figure 3.1: Basic Framework for Handover Analysis

.

The strategy of the whole process is shown in figure 3.1. In the following, these steps are explained for the specific scenario discussed above, starting from the computation of distances at different sample points from both Macro and Femto BS.

3.2 Distances for System Model

Here, we discuss the computation of distances from both macro and femto BSs. We begin with details of system model.

3.2.1 System Model

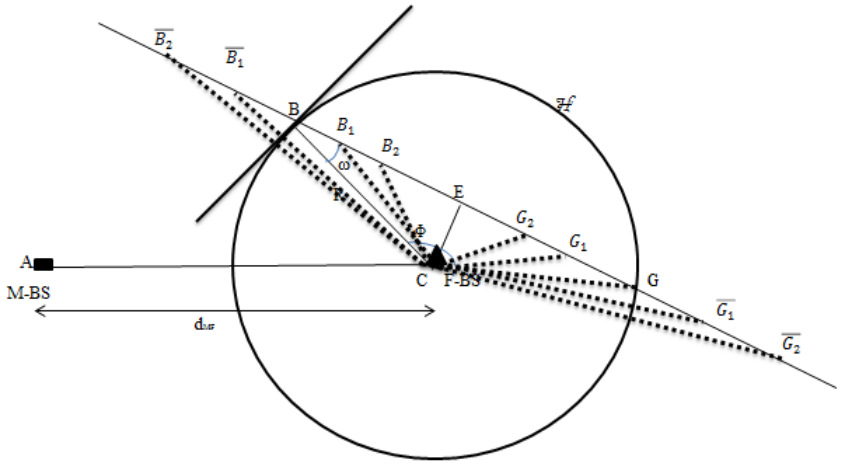

Figure 3.2: Reference Scenario

.

As discussed before, our model include one M-BS and one F-BS that are positioned at distance d_{MF}. We consider a specific situation where a UE moves with a constant speed v by following a straight line trajectory which creates an angle $\varnothing$ at the F-BS and crosses the border H of femto cell at point b by an incidence angle ω with respect to radius R of femto cell and a central angle ϕ from F-BS. If we

Table 3.1: Parameters used in System Model

Node	Transmit Power	Features
Macro base station	M-BS	(■)
Femto base station	F-BS	(▲)
Inter base distance	d_{MF}	200
Radius of femto cell	R	100
Incidence angle	ω	$(-\Pi/2, \Pi/2)$
Angular coordinate	ϕ	$(0, 2\Pi)$
Speed of light	c	$3 * 10^8 m/sec$

consider for a UE to enter femto cell from any point and with any angle, the values of ω & ϕ will vary in the range. The parameters and notations associated with the system model are mentioned in table 3.1.

3.2.2 Distances from F-BS

Distances can be computed from base station for any UE that enters its region. As mentioned earlier that UE can enter femto cell from any angle and from any point. In case, incidence angle ω is known, we can compute distances of the UE at different points inside the femto cell from the femto base station using following equations.

$$BE = BC \times \cos(\omega) \tag{3.2}$$

Here BE is half of the distance covered by the straight path inside femto cell boundary. Now to compute shortest distance of the straight path inside the femto cell from the femto base station, we have,

$$CE = BC \times \sin(\omega) \tag{3.3}$$

Here CE is the shortest distance from F-BS. If we divide the distance BE into N_L points and vary k from 1 to (N_L-1), we can compute each portion of the distance BE by using

$$BE_k = (N_L - k)\,(\frac{BE}{N_L}) \tag{3.4}$$

This means that, we can write

$$CB_k = \sqrt{(BE_k)^2 + (CE)^2} \tag{3.5}$$

where CB_k is the distance of the UE from F-BS for different values of k. N_L=Total number of sample points along the distance BE.

Next we discuss the computation of distances from the other half GE of the straight path of user equipment inside the femto boundary. It is observed that if we divide GE into N_L points, we will get mirror images of the distances CB_k as the distances CG_k for k=1,2,3...,N_L-1.

Now if we define $\overline{BE}$ as distance BE that is outside the femto cell on the straight path of the UE, we can divide $\overline{BE}$ into N_L points, and therefore,

$$\overline{CB}_k = \sqrt{\left(\left(\frac{N_L + k}{N_L}\right) BE\right)^2 + (CE)^2} \tag{3.6}$$

Analogous to the distances CG_k, we can compute $\overline{CG_k}$ that will be the mirror image of the distances $\overline{BE_k}$. All these distances of the UE path from the F-BS can be combined and stored as an array D_f.

3.2.3 Distances from M-BS

Analogous to the F-BS case, distances of user equipment from M-BS can be computed that lies in its region. Suppose, incidence angle ω is known and ϕ is in quadrant 2, that is ϕ =(90,180) than we can compute distances of the UE at different points as shown in Figure 3.3. We compute shortest distance AB by using Pythagoras theorem.

Sides that are unknown are computed by using side angle side formula,

$$s_{1_k} = \left(\frac{BE}{N_L}\right) \times k \tag{3.7}$$

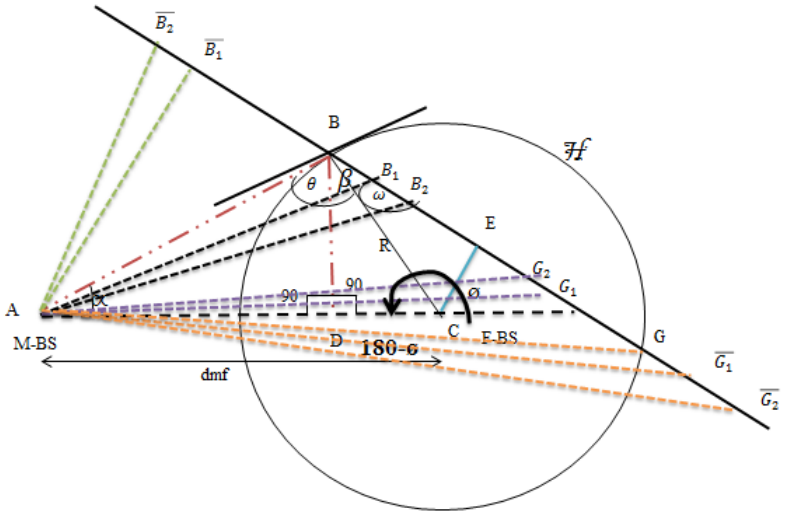

Figure 3.3: Quadrant 2, where $\phi = (90, 180)$

.

$$AB_k = \sqrt{(AB)^2 + (s_{1_k})^2 - 2 \times AB \times s_{1_k} \times cos\,(theta_b + \omega)} \tag{3.8}$$

If we define s_{2_k} as more than half of the distances inside the femto cell, that is,

$$s_{2_k} = \left(\frac{BE}{N_L}\right) \times (k + N_L) \tag{3.9}$$

then,

$$AG_k = \sqrt{(AB)^2 + (s_{2_k})^2 - 2 \times AB \times s_{2_k} \times cos\,(theta_b + \omega)}, \tag{3.10}$$

Also defining s_{3_k} as

$$s_{3_k} = \frac{BE \times (N_L - k + 1)}{N_L}, \tag{3.11}$$

$$\overline{AB}_k = \sqrt{(AB)^2 + (s_{3_k})^2 - 2 \times AB \times s_{3_k} \times cos\,(\pi - theta_b + \omega)} \tag{3.12}$$

It is easy to see that, for second and third quadrants,

$$theta_b = \theta + \pi/180 * \beta \tag{3.13}$$

$theta_b$ can be computed by using θ and β.

3.2.4 Distances with variation of ω and ϕ

In previous scenario, ϕ was in 2^{nd} quadrant and we compute all the distances from macro base station (M-BS). Now we will discuss computation of distances for different ω and ϕ.

For this, we need to find the shortest distance from M-BS to trajectory point. As we know that ϕ ranges from 0 to 360. So, we make cases out of it by dividing it into four quadrants and computing the respective unknown sides and angles as shown in the figure below.

Figure 3.4 and figure 3.5 shows the scenarios when ϕ =(0,90) and ϕ =(270,360),

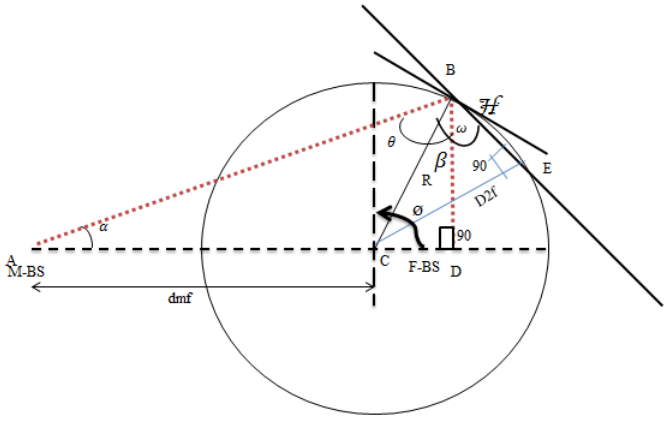

Figure 3.4: case1, when in quadrant 1, where $\phi = (0, 90)$

.

here AB is the distance from M-BS to the trajectory which needed to be compute for finding of d_m from M-BS to trajectory line. First we drew a perpendicular outside triangle ABC and make a right angled triangle out of it for computation of values. While figure 3.3, figure 3.7 shows scenarios when ϕ =(90,180), ϕ =(180,270), AB is the distance from M-BS to the trajectory which needed to be compute for finding of

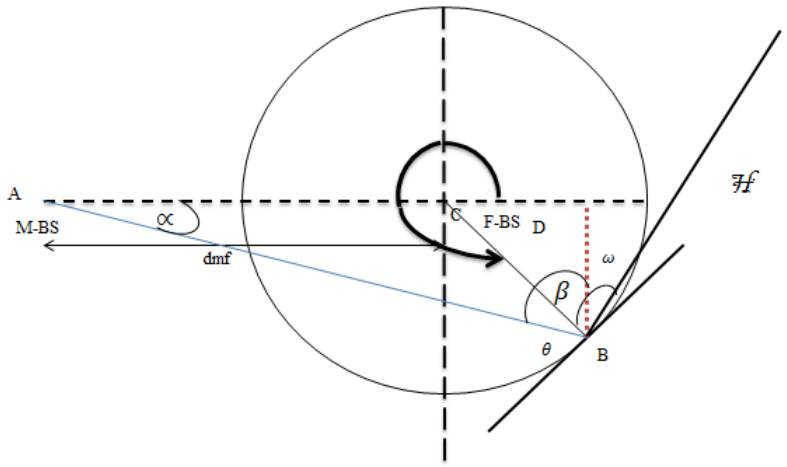

Figure 3.5: case 4 , when in quadrant 4, where $\phi = (270, 360)$

.

dm from M-BS to trajectory line. First we drew a perpendicular and make a right angled triangle BD out of it for computation of values.

From all the scenarios, we need to find BD and DC for all triangles. Out of which AD can be computed. α , β , θ can be computed out of all cases. Here,

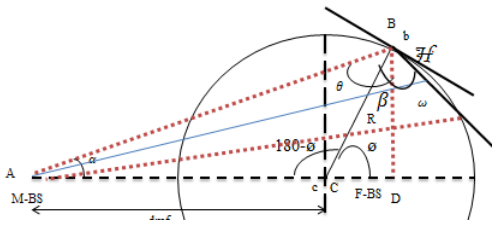

Figure 3.6: case 1a, when in quadrant 1, where $\phi = (0, 90)$

.

In case of first and fourth quadrant

$$theta_b = \gamma - \alpha \tag{3.14}$$

Now BCD is a right angled triangle, we compute the unknown sides and angles out of it and then from this we compute AB. Trigonometric functions are used in finding of unknown sides and angles. Other cases are shown in the figures below

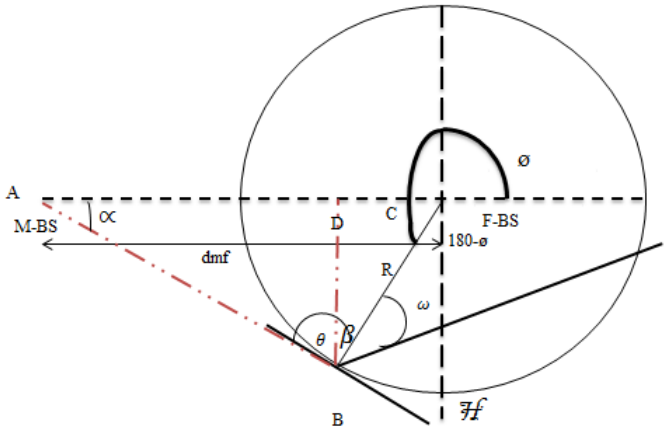

Figure 3.7: case 3, when in quadrant 3, where $\phi = (180, 270)$

.

Distances from M-BS can be computed from equation 3.10 to equation 3.12 with variation in the values of theta_b from equation 3.14 and equation 3.13 for their respective quadrants. After computing distances, we store s_1 s_2 and s_3 in an array i.e. $d_m = [s_3 \text{ AB } s_1 \ s_2]$.

3.3 Path Loss and RSS

After determining distances from M-BS and F-BS, distance dependent path loss can be computed. The difference (in dB) between the transmitted power and the received power is termed as pathloss.

Due to HetNets scenario, two diverse path loss models are implemented for dissimilar level UE$'s$. Distance dependent path loss model for macro cell UE can be expressed as

$$L_m = 128.1 + 37.6 \log 10 \, (d_m) \tag{3.15}$$

The distance d is in kms. L_m (in dB) is the path loss of k is at time slot t with macro cell M where m inside the subscript signifies the cell type is macro.

In a HetNet scenario [48], distance dependent for macro and femto cell should be

different. The path loss for femto is shown as follows

$$L_f = 140.7 + 36.7 \log 10 \, (d_f) \tag{3.16}$$

where f inside the subscript signifies the cell type is femto. Then, we define the incidence angle ω as the angle of UE and femto cell, the distance between macro and femto cell is expressed d_m and d_f as computed in previous sections. Here,

L_f=Path loss in dB for F-BS.

L_m =Path loss in dB for M-BS.

d_m= Distances of M-BS in km.

d_f= Distances of F-BS in km.

After computing distance dependent pathlosses, we can now calculate RSS for macro and femto cells.

The received signal strength (RSS) is defined as the capacity of power present in a received radio signal, that is typically measured in units of decibels (dB).

Using equation (3.15) and equation (3.16), the RSS of UE assigned to macro cell, at each time slot can be considered as

$$RSS_M = \frac{G_M^{tx}}{0.7 \times L_m} \tag{3.17}$$

where,

G_M^{tx} = Transmission power of M-BS

L_m = The distance dependent path loss of macro as computed in (3.15).

Similarly for femto BS,

$$RSS_F = \frac{G_F^{tx}}{0.36 \times L_f} \tag{3.18}$$

where,

G_F^{tx} = Transmission power of F-BS is in dBm,

L_f = The distance dependent path loss of femto as given in (3.16). computed above is in dB.

3.4 Handover and Markov Chain

Handover (HO) performance is driven by UEs prompt RSS. As we know that if SINR $< T_H$, HO takes place. If the difference between RSS of serving & target cells let consider one as F-BS and other as M-BS, falls below T_H value which is taken as 1 for both macro and femto BS falls below the HO threshold, countdown starts. If RSS becomes greater than threshold value, countdown that started at the point where RSS becomes greater than T_H value is aborted and HO is interrupted and stopped. On the contrary, if it remains less than threshold, UE disconnects. Whenever HO takes place it is neither connected to F-BS or M-BS. It is temporarily disconnected for HO to occur. This process continues for T_H time intervals and this switching process continues. RSS difference mentioned above can be considered equivalent to the SINR expression by UE, where interference is basically the power that is received from target cell. We are going to use this notation latter in the following sections.

3.4.1 State Probability using Markov Chain

At each step, UE starts moving along its trajectory and due to variation in SINR. As described previously that handover HO process starts when SINR < Threshold. States along with its steps are defined, as Markov chain state that is arrived when UE is attached to either F-BS or M-BS correspondingly and in this case SINR should remain below threshold for j succeeding steps. We then suppose that at some step k, MC is in state M_j. It evolves from M_j to M_{j+1}, if SINR < Threshold, otherwise the MC returns to M0 whatever step it is it will return back to zero state. On the contrary, if SINR remains lower than threshold when the MC is in state M_N, the

UE initiates the handover process to the F-BS and the MC arrives state H_1. In the following N_H steps the MC deterministically crosses all the handover states H_j and ends up in state F_0, regardless of the channel situations. At this instant, the UE is connected to F-BS, and the evolution of the MC is theoretically identical to that seen for the M_j states.

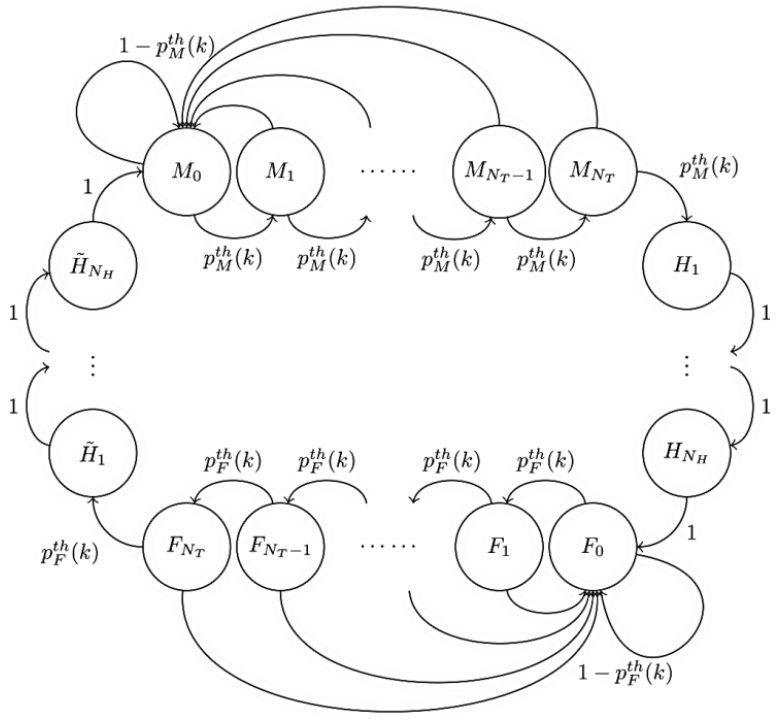

Figure 3.8: Non-homogenous discrete time Markov Chain

.

3.4.2 Transfer Probabilities

With the purpose of attaining the optimization standards for HetNets, probability formulation should be achieved from this Markov Chain Process. Consider a state that is M_1, which signifies that this state is associated to a macro cell. Its probability of moving to succeeding state is $P_M(x)$, In the meantime, while for moving back is $1 - P_M(x)$.

This similar rule relates for all macro states up to M_n transfer to H_1, which basically shows that handover is initiated. Within H states, it has 100% chance to move to subsequent state H till handover is terminated and after this UE has been transferred to femto cells, which is in state F_1. The guidelines for F and $H^{'}$ are the same for M and H states, so that whole Markov chain process loop is established.

One of the significant property for H and H$^{'}$ states is that the traffic signs plays a leading role to assure the handover process. Meanwhile, we have agreed upon all the states, we may be competent enough to construct transfer probability formula, which is $P_M(x)$ and $P_F(x)$ shown in equation below.

$$P_M(x) = \frac{\beta * RSS_{F,x}}{\alpha * RSS_{M,x} + \alpha * RSS_{F,x}} \tag{3.19}$$

$$P_F(x) = \frac{\beta * RSS_{M,x}}{RSS_{F,x} + \alpha * \beta * RSS_{M,x}} \tag{3.20}$$

Here x is the number of TTI.

In MCP, it shows the chance of continuing to check handover status. Providing UE received signals from both macro cells and femto cells, it will have the probability moving to the succeeding state till handover process. Consequently, we express our MCP transfer probability as follows.

Suppose there be a femto cell, UE stays in F state, it will obtain signals from macro cell R_{SS_M} but also from femto cell R_{SS_F}. These two signal power will strive to transfer UE from F states to $H^{'}$ states. When R_{SS_M} is the greater one, it will lead to that condition which has the purpose to initiate handover process and is unwilling to stay in femto cell network. The circumstances will be contradictory if (R_{SS_F}) is the larger one. At this point, HM bias and CRE bias will increase the weight of (R_{SS_F}) and oblige UE from moving back to macro cell, which is shown in equation 3.20. In equation 3.19 however they may possibly play the conflicting roles because CRE has additional purpose to offload UE$^{'}$s from macro cell to small one.

3.4.3 System Transition Matrix

Without any loss in the generality, we arrange states according to order M_j, H_j, F_j, $H_j^{'}$. System transition matrix P_k at the k-th step can then be expressed as.

$$P(k) = \begin{bmatrix} M(k) & V_M^H(k) & \phi & \phi \\ \phi & H(k) & V_H^F(k) & \phi \\ \phi & \phi & F(k) & V_F^{H'}(k) \\ V_{H'}^M(k) & \phi & \phi & H'(k) \end{bmatrix} \tag{3.21}$$

Where the submatrices M(k), H(k), F(k) , H (k) are in form of square transition matrices within the sets of Mj, H(j) , Fj, H (k) respectively. $V_{YX}(i)$ shows rectangular matrices. Elements of other blocks representing ϕ, are all equal to 0. ϕ shows null matrix having all elements as 0 in its all rows and columns.

3.4.4 Submatrices

Submatrix of P(k), M(k) is given by

$$M(k) = \begin{bmatrix} 1 - P_M(x) & P_M(x) & 0 & 0 \\ 1 - P_M(x) & 0 & P_M(x) & 0 \\ 1 - P_M(x) & 0 & 0 & P_M(x) \\ 1 - P_M(x) & 0 & 0 & 0 \end{bmatrix} \tag{3.22}$$

while for F(k) is given by

$$F(k) = \begin{bmatrix} 1 - P_F(x) & P_F(x) & 0 & 0 \\ 1 - P_F(x) & 0 & P_F(x) & 0 \\ 1 - P_F(x) & 0 & 0 & P_F(x) \\ 1 - P_F(x) & 0 & 0 & 0 \end{bmatrix} \tag{3.23}$$

while, H_j andH_j' are matrices that represents handover takes place from macro to femto and femto to macro handovers. It varies from H_1,H_2..... H_N. Size of H_k is:

$$H(k) = H'(k) = \begin{bmatrix} 0 & 1 & 0 & 0 \\ 0 & 0 & 1 & 0 \\ 0 & 0 & 0 & 1 \\ 0 & 0 & 0 & 0 \end{bmatrix} \tag{3.24}$$

Finally, $V_H^F(k)$ is rectangular transitions matrices from H to F while $V_H^M(k)$ are rectangular transition matrices from $H^{'}$ to M respectively as shown below

$$V_H^F(k) = V_H^M(k) = \begin{bmatrix} \phi & \phi \\ 1 & \phi \end{bmatrix} \tag{3.25}$$

Similarly, $V_M^H(k)$ and $V_F^H(k)$ are rectangular transition matrices from M to H and from F to H' respectively,

$$V_M^H(k) = \begin{bmatrix} \phi & \phi \\ P_M^{th}(k) & \phi \end{bmatrix} \tag{3.26}$$

$$V_F^H(k) = \begin{bmatrix} \phi & \phi \\ P_F^{th}(k) & \phi \end{bmatrix} \tag{3.27}$$

because matrix P (k) is of size 16 $\times$ 16. And all other matrices mentioned above are the matrices that lie inside P (k). Block matrix condition is being used so for that size of all matrices inside P (k) are of same size, hence; it will give matrices by substituting in P (k). State probability vector p(k) at kth stage is assumed by:

3.4.5 Markov Transfer Matrix

Transfer matrix T can be attained after Markov chain process and its transition probability is definite, UEs HO process affecting by HM and CRE is customary. Figure 3.9 shows the transfer probability used in our simulation, it is a 4-state transfer matrix.

	M0	M1	M2	M3	H0	H1	H2	H3	F0	F1	F2	F3	H'0	H'1	H'2	H'3
M0	$1-P_M(x)$	$P_M(x)$	0	0	0	0	0	0	0	0	0	0	0	0	0	0
M1	$1-P_M(x)$	0	$P_M(x)$	0	0	0	0	0	0	0	0	0	0	0	0	0
M2	$1-P_M(x)$	0	0	$P_M(x)$	0	0	0	0	0	0	0	0	0	0	0	0
M3	$1-P_M(x)$	0	0	0	$P_M(x)$	0	0	0	0	0	0	0	0	0	0	0
H0	0	0	0	0	0	1	0	0	0	0	0	0	0	0	0	0
H1	0	0	0	0	0	0	1	0	0	0	0	0	0	0	0	0
H2	0	0	0	0	0	0	0	1	0	0	0	0	0	0	0	0
H3	0	0	0	0	0	0	0	0	1	0	0	0	0	0	0	0
F0	0	0	0	0	0	0	0	0	$1-P_F(x)$	$P_F(x)$	0	0	0	0	0	0
F1	0	0	0	0	0	0	0	0	$1-P_F(x)$	0	$P_F(x)$	0	0	0	0	0
F2	0	0	0	0	0	0	0	0	$1-P_F(x)$	0	0	$P_F(x)$	0	0	0	0
F3	0	0	0	0	0	0	0	0	$1-P_F(x)$	0	0	0	$P_F(x)$	0	0	0
H'0	0	0	0	0	0	0	0	0	0	0	0	0	0	1	0	0
H'1	0	0	0	0	0	0	0	0	0	0	0	0	0	0	1	0
H'2	0	0	0	0	0	0	0	0	0	0	0	0	0	0	0	1
H'3	1	0	0	0	0	0	0	0	0	0	0	0	0	0	0	0

Figure 3.9: Markov Transfer Matrix

$$V_x = V_i \prod_{i=1}^{x} T(i) \tag{3.28}$$

In Equation 3.28, the V_1 is the probability of UEs initial state, which states as 1. e.g. if the state M_1 is in time 1, then its probability vector can be written as $[1, 0, 0, ..., 0]$. With the increase in its TTI, UE is moving which causes its probability $P_m(x)$ and $P_s(x)$ to change in the Markov Transfer Matrix (T), according to Equation 3.28. The vector for any UE at any step x can be computed, so that the HOR can be assessed.

Chapter 4

Results & Discussions

In this chapter, simulation results are presented to analyse handover performance (HO) under different combinations. All simulations are performed in MATLAB. The simulated parameters are summarized in Figure 4.1.

As mentioned in Chapter 3, our system model include M-BS and F-BS that are positioned at distance d_{MF}, radius R. UE moves by following a straight trajectory creating an angle ϕ and crosses border H of femto cell at point b by an incidence angle ω.

Figure 4.1 is a reference scenario where a linear trajectory is being monitered by

Table 4.1: Parameters used in Pathloss computation

Parameters	Values
Time step (S_T)	1-31
Radius (R)	100m
Incidence angle ω	$(-\Pi/2, \Pi/2)$
Angular coordinate ϕ	$(0, 2\Pi)$
Pathloss (Lf)	140.7+36.7 log_{10} d_f
Pathloss (Lm)	128.1+37.6 log_{10} d_m

a UE when arriving the femto cell at point b through handover line H with diverse incidence angle ω. In the figure, we consider values of ω to be 25^o, 35^o, 45^o, 55^o, 65^o that are used to compute pathlosses along these trajectories with θ considered in all

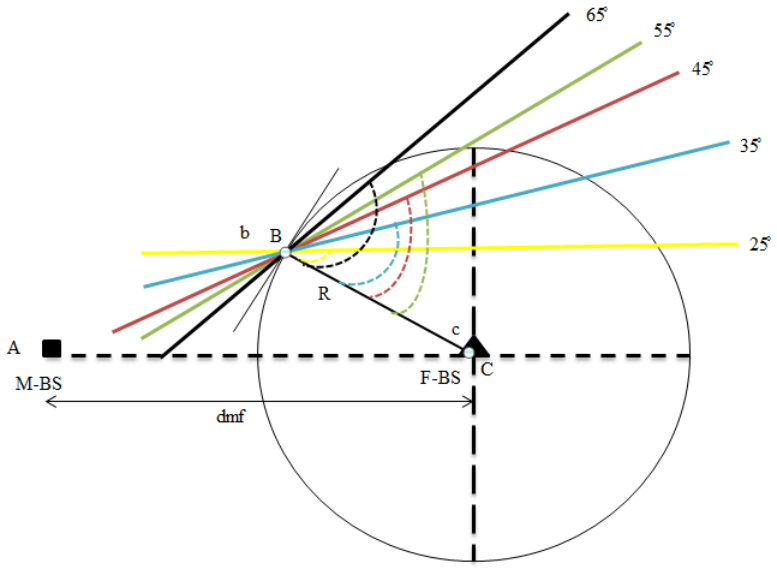

Figure 4.1: Reference scenario: Linear trajectory monitored by a UE when arriving the femto cell at point b with diverse incidence angles ω

four quadrants.

As mentioned in Chapter 3 , the first step is to compute distances. Here, we calculate distances for different incidence angles ω and for different θ as given in Table 4.2 , Table 4.3 and Table 4.4.

Table 4.2 shows distances of the UE from F-BS for different ω the values in d_f. There is a mirror image in the values of the distances after N_L points which is fixed to 10. Similarly for macro cell, distances are computed at different ω and ϕ in all four quadrants. Table 4.3 shows distances from M-BS when UE is in quadrant 2 and quadrant 3.

Knowing all the distances, we can compute the corresponding path losses. Figure 4.2 shows how pathloss of the femto base station (F-BS) is varying under different values of time step S_t. X-axis is labeled as time step S_t and Y-axis is labeled as pathloss L_f. In general, it can be observed that pathloss for F-BS will reduce and is very less when incidence angle is small i.e. 25^o. However their influence may

Table 4.2: Distances of F-BS obtained under different ω

	ω=25	ω=35	ω=45	ω=55	ω=65
Sr.No.	df	df	df	df	df
1	186.12	173.58	158.11	140.95	123.92
2	177.30	165.87	151.82	136.33	121.08
3	168.52	158.21	145.60	131.79	118.32
4	159.76	150.60	139.46	127.34	115.65
5	151.04	143.06	133.41	123.01	113.07
6	142.36	135.60	127.47	118.79	110.60
7	133.73	128.22	121.65	114.70	108.23
8	125.17	120.95	115.97	110.77	105.98
9	116.67	113.80	110.45	106.99	103.85
10	108.28	106.81	105.11	103.39	101.85
11	100.00	100.00	100.00	100.00	100.00
12	91.86	93.40	95.13	96.82	98.28
13	83.92	87.08	90.55	93.89	96.73
14	76.22	81.10	86.31	91.22	95.33
15	68.87	75.53	82.46	88.85	94.11
16	61.96	70.48	79.05	86.79	93.06
17	55.68	66.05	76.15	85.06	92.19
18	50.25	62.40	73.82	83.70	91.51
19	45.98	59.65	72.11	82.71	91.02
20	43.22	57.93	71.06	82.11	90.72
21	42.26	57.35	70.71	81.91	90.63
22	43.22	57.93	71.06	82.11	90.72
23	45.98	59.65	72.11	82.71	91.02
24	50.25	62.40	73.82	83.70	91.51
25	55.68	66.05	76.15	85.06	92.19
26	61.96	70.48	79.05	86.79	93.06
27	68.87	75.53	82.46	88.85	94.11
28	76.22	81.10	86.31	91.22	95.33
29	83.92	87.08	90.55	93.89	96.73
30	91.86	93.40	95.13	96.82	98.28
31	100.00	100.00	100.00	100.00	100.00

Table 4.3: Distances of M-BS obtained under different ω in 1st and 4th quadrant

	ω=25	ω=35	ω=45	ω=55	ω=65
Sr.No.	dm	dm	dm	dm	dm
1	312.73	295.42	278.71	264.90	256.24
2	307.05	291.45	276.51	264.31	256.77
3	301.54	287.65	274.48	263.84	253.37
4	296.20	284.04	272.62	263.49	258.04
5	291.04	280.63	270.93	263.27	258.78
6	286.08	277.41	269.42	263.18	259.58
7	281.33	274.40	268.08	263.21	260.45
8	276.79	271.61	266.93	263.36	261.38
9	272.48	269.03	265.96	263.64	262.38
10	268.40	266.69	265.71	264.04	263.44
11	264.57	264.57	264.57	264.57	264.57
12	261.00	262.69	264.16	265.22	265.76
13	257.70	261.06	263.93	265.99	267.01
14	254.68	259.68	263.90	266.89	268.32
15	251.95	258.54	264.06	267.90	269.69
16	249.51	257.67	264.40	269.03	271.12
17	247.39	257.05	264.93	270.28	272.61
18	245.58	256.69	265.65	271.64	274.15
19	244.10	256.59	266.56	273.12	275.75
20	242.94	256.76	267.65	274.71	277.41
21	242.12	257.18	268.92	276.41	279.12
22	241.64	257.87	270.37	278.22	280.88
23	241.50	258.81	272.00	280.13	282.70
24	241.69	260.01	273.80	282.15	284.56
25	242.23	261.46	275.76	284.27	286.48
26	243.10	263.15	277.90	286.49	288.45
27	244.31	265.09	280.20	288.80	290.46
28	245.84	267.26	282.65	291.21	292.52
29	247.70	269.67	285.26	293.71	294.63
30	249.87	272.30	288.02	296.30	296.78
31	252.35	275.15	290.93	298.98	298.98

Table 4.4: Distances of M-BS obtained under different ω in 2nd and 3rd quadrant

	ω=25	ω=35	ω=45	ω=55	ω=65
Sr.No.	dm	dm	dm	dm	dm
1	30.65	29.88	42.16	59.06	76.26
2	36.71	37.96	48.90	63.90	79.47
3	43.81	40.07	55.72	68.89	82.76
4	51.54	54.21	62.59	73.99	86.14
5	59.64	62.37	69.51	79.17	89.59
6	67.98	70.53	76.45	84.42	93.10
7	76.49	78.70	83.41	89.73	96.67
8	85.12	86.87	90.39	95.10	100.29
9	93.82	90.05	97.39	100.50	103.95
10	102.59	103.23	104.39	105.94	107.66
11	111.41	111.41	111.41	111.41	111.41
12	120.26	119.59	118.43	116.90	115.18
13	129.14	127.77	125.45	122.42	118.99
14	138.04	135.95	132.48	127.95	122.83
15	146.97	144.14	139.52	133.50	126.69
16	155.91	152.33	146.55	139.07	130.57
17	164.86	160.51	153.59	144.65	134.47
18	173.83	168.70	160.64	150.24	138.39
19	182.80	176.89	167.68	155.84	142.33
20	191.79	185.07	174.73	161.46	146.29
21	200.78	193.26	181.78	167.08	150.26
22	209.77	201.45	188.83	172.10	154.24
23	218.77	209.64	198.89	178.34	158.24
24	227.78	271.83	202.94	183.98	162.25
25	236.79	226.02	210.00	189.63	166.27
26	245.81	234.20	217.05	198.28	170.30
27	254.83	242.39	224.11	200.94	174.34
28	263.85	250.58	231.17	206.60	178.38
29	272.87	258.77	238.23	212.26	182.44
30	281.90	266.96	245.29	217.93	186.50
31	290.93	275.15	252.35	223.60	190.57

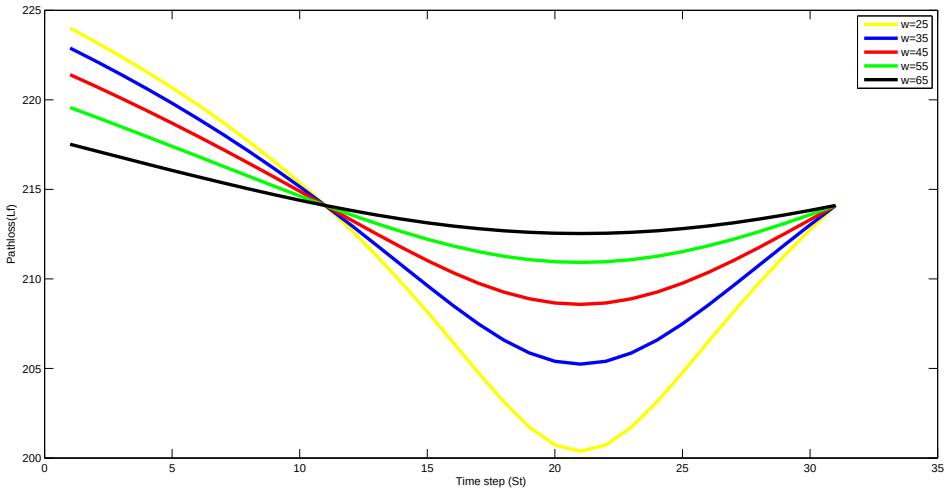

Figure 4.2: Path loss of F-BS obtained under different ω with θ at all quadrants, as a function of time step T

differ in many aspects. For example, firstly we consider incidence angle to 25^o. At this point, it is close to femto, having shorter distance values its pathloss reduces because it is close to the radius of the circle which is at (F-BS). Its shortest distance is shortest comparable to other values of incidence angle. As soon as incidence angle starts increasing, distance increases due to which pathloss starts increasing. As we approach to incidence angle of 90^o, the UE moves away from femto base station and its distances increases due to which pathloss increases. In Figure 4.2, we take maximum incidence angle to be 65^o. Its shortest distance is greater than that at 25^o. We also consider different values of θ in ω all four quadrants to evaluate pathloss, but in case F-BS, it has no effect on pathloss because the distances of F-BS has no dependency on variation of θ. In all four quadrants for θ, its curves and pathloss effect remains same for all four quadrants.

Figure 4.3 shows how pathloss of macro base station(M-BS) under different ω with θ in all four quadrants varies as a function of time step S_t. At small value of incidence angle i.e. 25^o, the UE is far from M-BS and its pathloss is smallest.

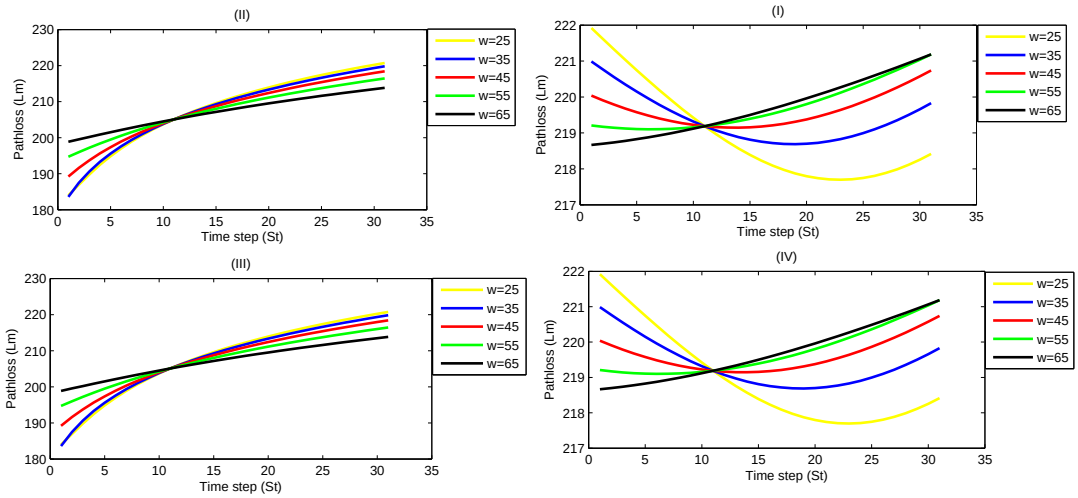

Figure 4.3: Path loss of M-BS obtained under different ω at all four quadrants, as a function of time step T

As soon as ω increases, its distances starts reducing and it comes near to M-BS there is an increase in the value of pathloss. A point will reach where it starts reaching to a straight line. With the variation in ϕ it has effect in its pathloss with respect to ω. We consider θ in all four quadrants to check its behaviour. Figure 4.3 presents the graphs of pathloss in four different quadrants.

Figure 4.3(i) (iv) shows when θ is in 1^{st} and 4^{th} quadrant and they are same results along with mirror image of these two quadrants that when ω is 25^o, away from M-BS and pathloss is good and is smallest as it approaches to greater angle i.e. 65^o pathloss starts increasing as distance increases respectively.

Figure 4.3 (ii), (iii) shows the results in 2^{nd} and 3^{rd} quadrant, mirror image is created,when ω is 25^o its pathloss is very large as its distance from M-BS is larger but gradually with the increase in ω path loss starts reducing as it comes near to base station.

4.1 Received Signal Strength

Let us see the received signal strength for femto cell in figure 4.4 that shows RSS of femto base station (F-BS) is obtained under different ω, independent of θ, as a function of time step S_t. X-axis is labled as time step (S_t) and Y-axis is labeled as received signal strength (RSS).

Generally speaking, it can be concluded that RSS for F-BS will decrease as incidence angle approaches to 90^o. At start point when incidence angle is 25^o. At this point it is closer to radius and femto base station, distance is short due to which signal strength is good. As soon as ω starts increasing, it starts moving away from F-BS due to which distances increases that causes signal strength to become weak and poor as approaches to 90^o and its curves starts to become a straight line. This case is observed for all values of θ. The effect of RSS remains same in all four quadrants as femto is independent of θ.

Figure 4.5 (i), (iv) shows RSS effects in 1^{st} and 4^{th} quadrant. It shows received

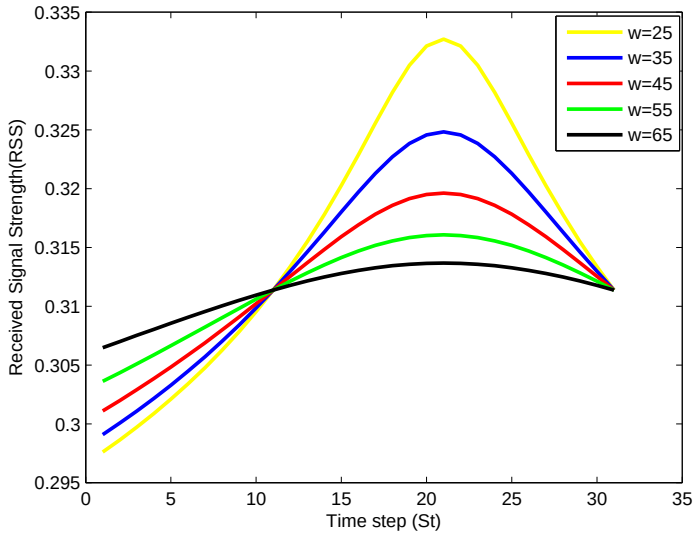

Figure 4.4: Received signal strength of F-BS obtained under different ω at all four quadrants, as a function of time step T

signal strength of macro base station (M-BS) which is obtained under different ω, θ, as a function of time step T. X-axis is labeled as time step S_t. Y-axis is labeled as received signal strength (RSS).

Generally speaking, it can be concluded that RSS for M-BS will starts decreasing as there is an increase in incidence angle as it comes closer to M-BS. A point will reach when a straight line is achieved and received signal strength becomes constant.

Figure 4.5 (ii), (iii) shows RSS effects in 2^{nd} and 3^{rd} quadrant. It shows received signal strength of macro base station (M-BS) which is obtained under different ω, θ , as a function of time step T. X-axis is labeled as time step (T) and Y-axis is labeled as received signal strength (RSS). Generally speaking, it can be concluded that RSS for M-BS will start increasing as there is an increase in incidence angle. Thus as it approaches to 90^o it gives us a straight line. In beginning, RSS is weak and it becomes stronger as it approches to maximum value of ω.

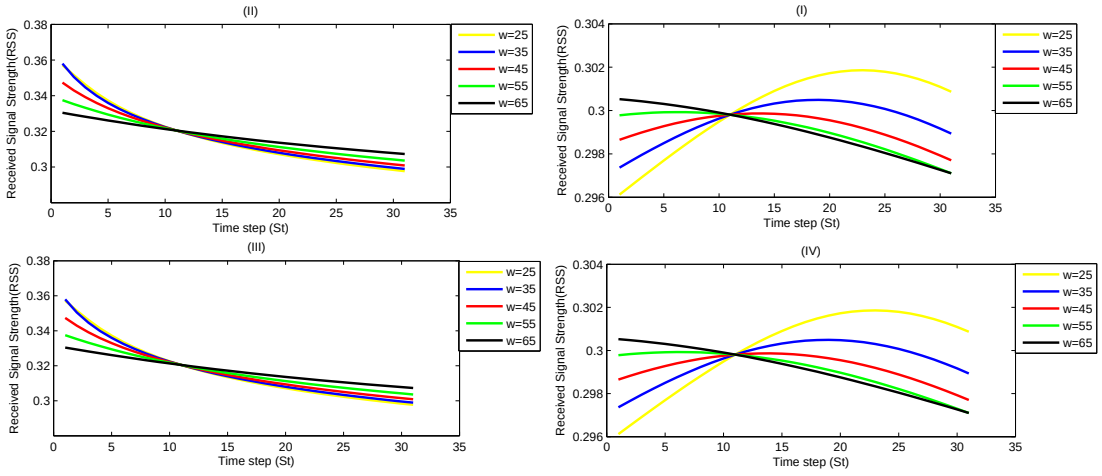

Figure 4.5: Received signal Strength of M-BS obtained under different ω as a function of time step T

4.2 Markov Chain & State Transitions

Transfer Matrix T can be attained after the MC process and its transition probability is defined; then, the model of UEs handover process affects by probability states is established. Figure 3.9 listed the transfer probability used in our simulation, it is a 4-state transfer matrix. After the set up of probability transfer matrix, calculations of state probability vector can be done by Equation 3.28. In Equation 4.1, the pn0 is the probability of UEs initial state, which is expressed as 1 in the vector.

With the TTI increases, the UE is moving, which will cause the probability $P_M(x)$ and $P_F(x)$ changing in the Markov Transfer Matrix (T), according to equation 4.1, the vector pn0 will also change.

Next state 2 gives us M2= 0.50 and M3= 0.49 which means that either it will remain in that particular state or moves forward and this goes on till it reaches to H^{th} state where handover starts from macro to handover state and condition for handover will be checked.

$$pn0 = \begin{bmatrix} 1 & 0 & ..... & 0 & 0 \end{bmatrix} \tag{4.1}$$

4.3 Handover rate Variations w.r.t paramters

Figure 4.7 , Figure 4.8 shows handover rate (HOR) react to hysteresis margin (HM) and cell range expansion (CRE) at different TTT's while increasing number of states when they are in 1^{st} quadrant. It can be determined at this point that both HM and CRE will decrease handover rate as the number of states and HM/CRE increases. We compute HOR by multiplying state transition vector and system transition matrix. However their impact mark might vary in numerous phases. Firstly the effect

	M0	M1	M2	M3	H0	H1	H2	H3	F0	F1	F2	F3	H'0	H'1	H'2	H'3
M0	0.510	0.489	0	0	0	0	0	0	0	0	0	0	0	0	0	0
M1	0.510	0	0.489	0	0	0	0	0	0	0	0	0	0	0	0	0
M2	0.510	0	0	0.489	0	0	0	0	0	0	0	0	0	0	0	0
M3	0.510	0	0	0	0.489	0	0	0	0	0	0	0	0	0	0	0
H0	0	0	0	0	0	1	0	0	0	0	0	0	0	0	0	0
H1	0	0	0	0	0	0	1	0	0	0	0	0	0	0	0	0
H2	0	0	0	0	0	0	0	1	0	0	0	0	0	0	0	0
H3	0	0	0	0	0	0	0	0	1	0	0	0	0	0	0	0
F0	0	0	0	0	0	0	0	0	0.489	0.510	0	0	0	0	0	0
F1	0	0	0	0	0	0	0	0	0.489	0	0.510	0	0	0	0	0
F2	0	0	0	0	0	0	0	0	0.489	0	0	0.510	0	0	0	0
F3	0	0	0	0	0	0	0	0	0.489	0	0	0	0.510	0	0	0
H'0	0	0	0	0	0	0	0	0	0	0	0	0	0	1	0	0
H'1	0	0	0	0	0	0	0	0	0	0	0	0	0	0	1	0
H'2	0	0	0	0	0	0	0	0	0	0	0	0	0	0	0	1
H'3	1	0	0	0	0	0	0	0	0	0	0	0	0	0	0	0

Figure 4.6: Markov Transfer Matrix

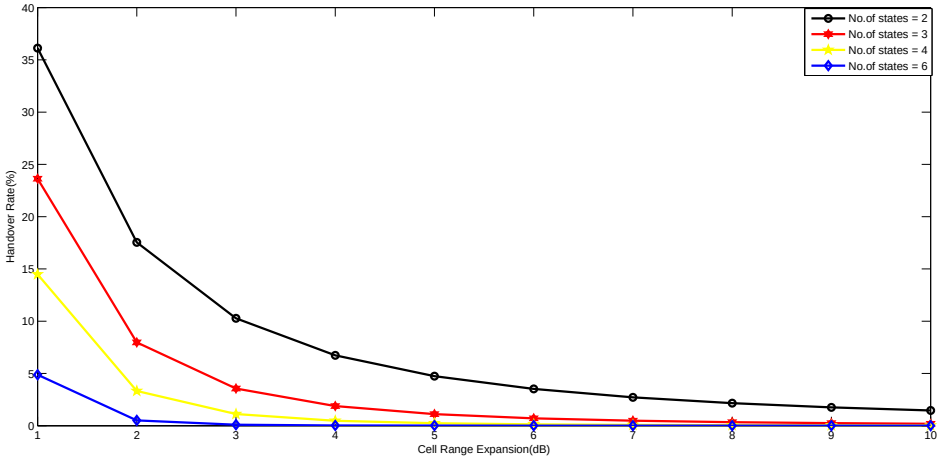

Figure 4.7: Handover Rate vs CRE obtained under different ω and when θ is in 1st quadrant

of HM of 1st quadrant is judged. Here X-axis shows HM which ranges from 1-10 dB. While Y-axis shows handover rate. $HM^{'}s$ effect on handover rate keeps on increasing. As approaching to maximum states, handover rates becomes minimum Effect of $HM^{'}s$ effect on handover rates keeps growing and attain the limitation. Furthermore, the starting and ending point of CRE and HM varies from one another. Outcome of CRE declines quickly and can be neglected, where HO rate stands still. HM can reduce handover rate from 38.89% to 0% while CRE can make it around

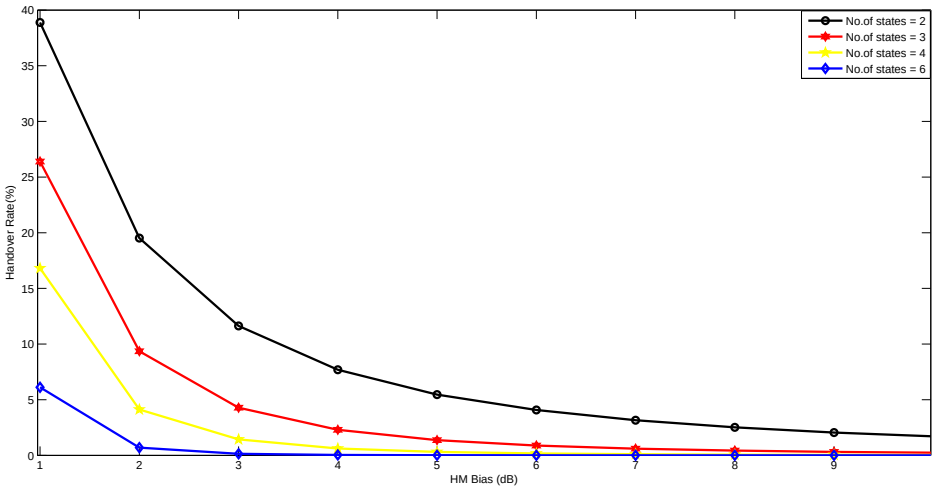

Figure 4.8: Handover Rate vs HM obtained under different ω and when θ is in 1st quadrant

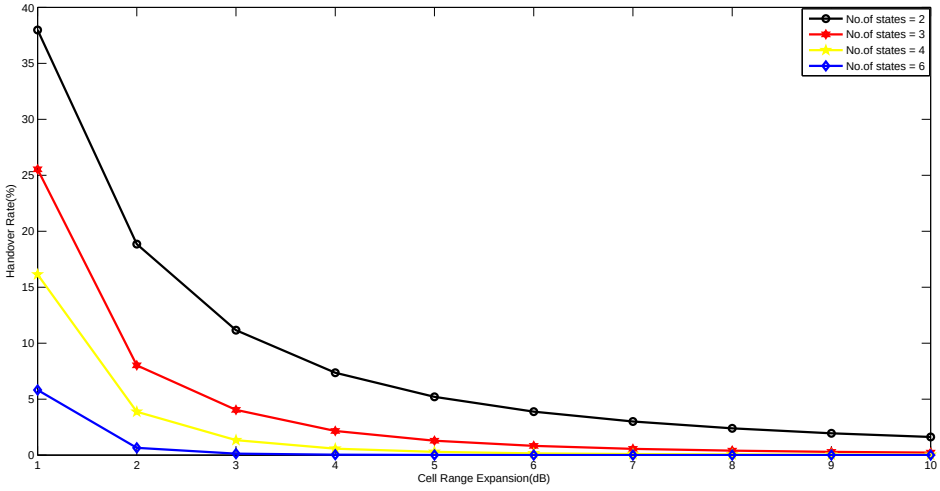

Figure 4.9: Handover Rate vs CRE obtained under different ω and when θ is in 2nd quadrant

0.002%. All these occurrences show the dominance of HM in handover control. Reason may be obtained from MCP probability formula and physical meanings of two parameters.$HM^{'}s$ main purpose is delay HO process and assure the UE$^{'}$ to their allocated cells, which includes both M and F cell. On the other hand, CRE has additional purpose to offload the UE's from macro to femto cell.

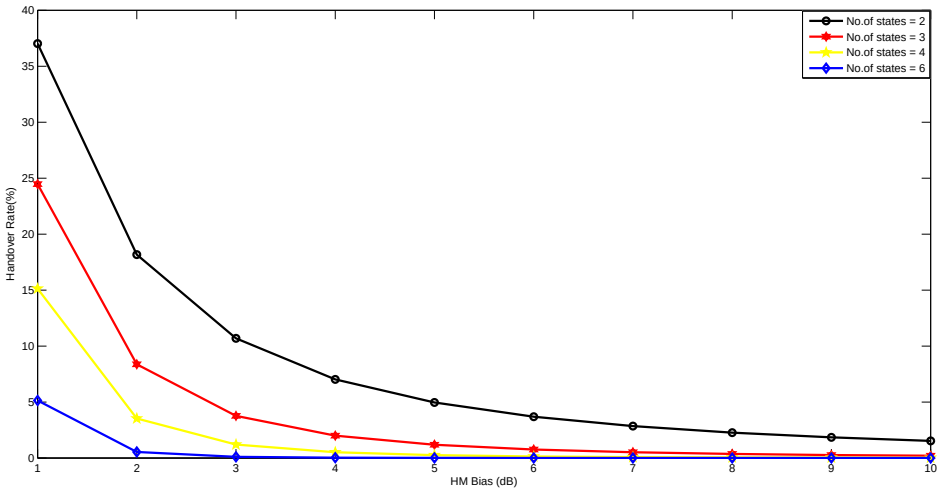

Figure 4.10: Handover Rate vs HM obtained under different ω and when θ is in 2nd quadrant

Consequently, CRE and HM may perhaps take reverse effects on handover rate when UE's try to handover from macro cell to small cell.

It also clarifies why handover rate will still persist 0.002% no matter what CRE

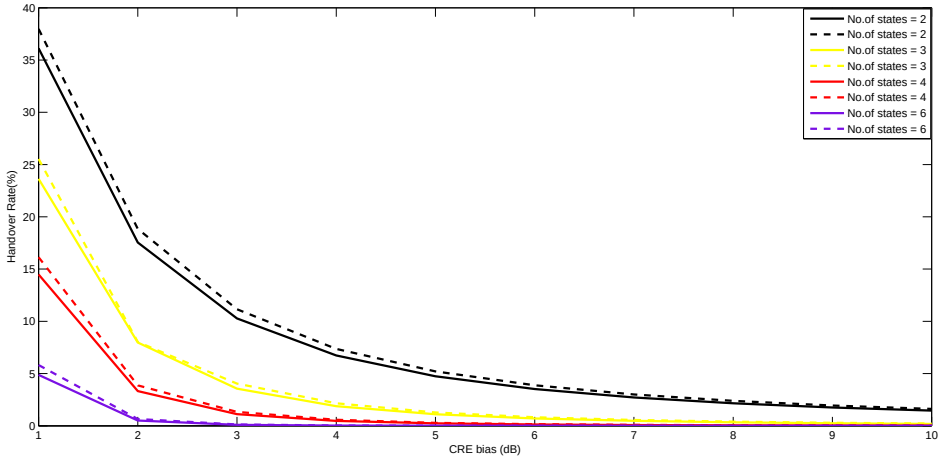

Figure 4.11: Comparison of Handover Rate vs CRE obtained under different ω and when θ in 1st and 2nd quadrants

value the network takes. Though, HMs effect on growing total quantity is incomplete due to its deficiency of offloading effect in HetNets network. Its prompt effect

of handover control also limits that HM bias may not reach a large value. Hence, an optimal arrangement of CRE and HM value is obligatory for HetNets network. Figure 4.9 and Figure 4.10 tells us the effect of HOR in 2nd quadrant. We analyze

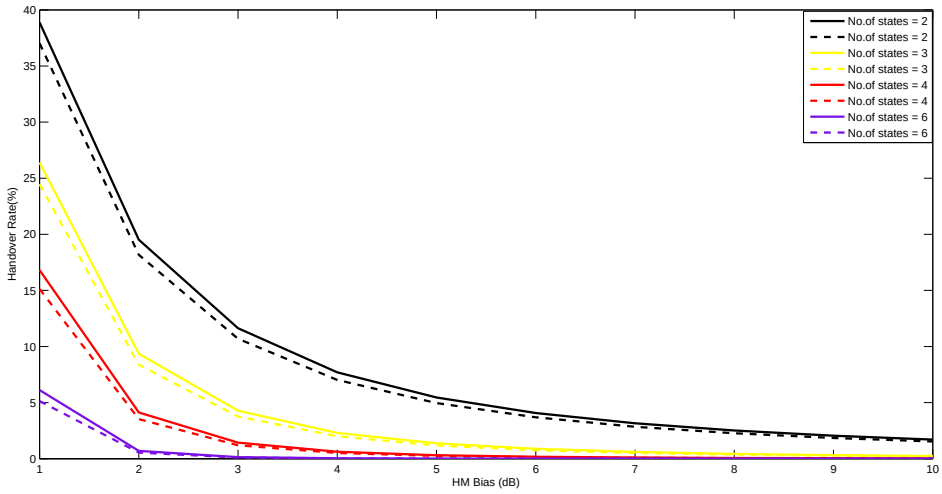

Figure 4.12: Comparison of Handover Rate vs HM obtained under different ω and when θ in 1st and 2nd quadrants

it in its same way. Effect of HM/CRE in 2nd quadrant is judged. Here X-axis shows HM/CRE which ranges from 1-10 dB. While Y-axis shows Hand over rate. Effect of HO rate on HM keeps on growing. HM can reduce HO rate from 37.02% to 0% while CRE can make it around 0.003%. All occurrences show the dominance of HM. As approaching to maximum states, handover rates becomes minimum approaches to zero

Figure 4.11 and Figure 4.12 shows the comparison of HM and CRE in 1st and 2nd quadrants. Existing model tells us in particular margin we study from different angles, we get more or less almost similar graphs of CRE and HM. Their behavior is almost same.

Let say, there be any value in state vector pn i.e. P=(P_{M1}, P_{M2}, P_{M3}, P_{M4}, P_{I1}, P_{I2} P_{I1} P_{I4}.....). If in these P_{I1}, P_{I2} P_{I1} P_{I4} any value exists . HO must occur as

soon as probabilities becomes non-zero which means that there is a chance of HO to occur and tells us HO rate. It also tells us that after how many steps we will obtain non-zero at HO places in terms of TTI. These non-zeros places after steps shows TTI and each step represents one TTI.

Chapter 5

Conclusion and Future Work

5.1 Conclusion

Modeling and simulation of heterogeneous communication networks using Markov based framework for handover process has been performed. A particular HetNet from the literature has been utilized where the handover process of a user equipment between a macro and a femto cell is discussed. It is assumed that the UE is initially moving in the macro cell and then start moving in a straight line towards the femto cell. Dividing the path of UE in some discrete portions and representing each part as a state, we model this process through Markov Chain. The effect of variations in incidence angle on the boundary of femto cell and in the angle of arrival at the femto cell base station has been incorporated in the Markov Chain. Under these variations, we observed the role of hysteresis margin (HM) and cell range expansion (CRE) on the handover rate. It is observed that for a fixed value of CRE, increase in HM reduces the handover rate to a very small value and vice versa.

5.2 Future Work

In future, this work can be extended by implementing more parameters to improve handover results. HATA model is used in this research, other models can be used

depending on scenarios. Number of UE$'$s can be increased in future research to check its impact on proposed algorithm.

Bibliography

[1] CISCO, " CISCO visual networking index: Global mobile data traffic forecast update, 2015-2020", 2015.

[2] D. Lopez-Perez, I.Guvenc, G.de la Roche, M.Kountouris, T.Quek, and J.Zhang, "Enhanced intercell interference coordination challenges in heterogeneous networks", Wireless Communications, IEEE, vol. 18, no. 3, pp. 22-30, June 2011.

[3] E.Hossain, M.Rasti, H.Tabassum, and A.Abdelnasser, "Evolution towards 5g multi-tier cellular wireless networks: An interference management perspective", CoRR, vol. abs/1401.5530, 2014.

[4] T.Korkmaz and M.Krunz, "Multi-constrained optimal path selection", in INFOCOM 2001. Twentieth Annual Joint Conference of the IEEE Computer and Communications Societies. Proceedings. IEEE, vo000l. 2, pp. 834-843 2001.

[5] J.Andrews, "Seven ways that HetNets are a cellular paradigm shift", IEEE Communications Magazine, vol. 51, no. 3, pp.136-144, March 2013.

[6] S.Podlipnig and L.Boszormenyi, "A survey of web cache replacement strategies", ACM Computer Survey, vol.35, no.4, pp.374-398, Dec.2003.

[7] G.Giannattasio, A Guide to the Wireless Engineering Body of Knowledge (WEBOK). WILEY, 2009.

[8] A.Taha, N.A.Ali and H.S.Hassanein, LTE-Advanced and WiMAX, 1st ed. UK: Wiley, 2012.

[9] F.Zhu and J.McNair, " Optimizations for vertical handover decision algorithms", IEEE Wireless Communications and Networking Conference (WCNC 2004), vol.2, pp.867-872, 2004.

[10] Qualcomm Incorporated, "LTE Advanced: Heterogeneous networks," white paper, Jan. 2011.

[11] A.Damnjanovic, J.Montojo, Y.Wei, T.Ji, T.Luo, M.Vajapeyam, T.Yoo, O.Song, and D.Malladi, "A survey on 3GPP heterogeneous networks", IEEE Wireless Commun. Mag., vol. 18, no. 3, pp. 10-21, June 2011.

[12] I.F.Akyildiz, J.McNair, J.S.M.Ho, H.Uzunalioglu, W.Wang, "Mobility management in next-generation wireless systems", Proceedings of the IEEE, vol. 87, no. 8, pp. 1347-1384, August 1999.

[13] A.H.Zahran, B.Liang, and A.Saleh, "Signal threshold adaptation for vertical handover inheterogeneous wireless networks", Mobile Networks and Applications, vol. 11, no. 4, pp. 625-640,August 2006.

[14] S.Balasubramaniam and J.Indulska, "Vertical handover supporting pervasive computing in futurewireless networks", Computer Communications, vol. 27, no. 8, pp. 708-719, 2004.

[15] J.G.Andrews,"Seven ways that HetNets are a cellular paradigm shift", IEEE Commun. Mag., vol.51, no.3, pp.136-144, March 2013.

[16] T.Ahmed, K.Kyamakya and M.Ludwig, "Design and Implementation of a Context Aware Decision Algorithm for Heterogeneous Networking", ACMSAC'06.

[17] M.Peng, D.Liang, Y.Wei, J.Li, and H.Chen, "Self-configuration and self-optimization in LTE-Advanced heterogeneous networks", IEEE Communications Magazine, vol.51, no.5, pp.36-45, May 2013.

[18] K.Yang, I.Gondal, and B.Qiu, "Context Aware Vertical Soft Handover Algorithm for heterogeneous wireless networks", in Proc.VTC Fall, pp.1-5, 2008.

[19] 3GPP TR 36.839, "Evolved universal terrestrial radio access (E-UTRA); Mobility enhancements in heterogeneous networks (Release 11)", version 11.0.0, Sep. 2012.

[20] D.Xenakis, N.Passas, L.Merakos, and C.Verikoukis, "Mobility management for femto cells in LTE-advanced: Key aspects and survey of handover decision algorithms", IEEE Communications Surveys Tutorials, vol.16, no.1, pp.64-91, 2014.

[21] R.Tawil, J.Demerjain, G.Pujolle and O.Salazar, "Processing-Delay Reduction During The Vertical Handover Decision In Heterogeneous Wireless System", International Conference on Computer Systems and Applications, AICCSA IEEE/ACS 2008, pp.381-385.

[22] D.J.Deng, H.C.Yen,"Quality-of-Service provisioning system for multimedia transmission" in IEEE802.11 wireless LANs, IEEE Journal on Selected Areas in Communication 23 vol.6, pp.1240-1252, 2005.

[23] H.S.Park, H.S.Yoon, T.H.Kim, J.S.Park, M.S.Duo and J.Y.Lee, "Vertical handover procedure and algorithm between IEEE802.11 WLAN and CDMA cellular network", Mobile Communications pp.103-112 2003.

[24] 3GPP TR 36.839, "Evolved universal terrestrial radio access (E-UTRA); Mobility enhancements in heterogeneous networks (Release 11)", version 11.0.0, Sep. 2012.

[25] F.Guidolin, I.Pappalardo, A.Zanella and M.Zorzi, "Context-aware handover policies in HetNets", IEEE Trans. Wireless Commun., vol.15,no.3, pp.1895-1906, March 2016.

[26] D.Lopez-Perez, I.Guvenc, and X.Chu, "Theoretical analysis of handover failure and ping-pong rates for heterogeneous networks", in IEEE International Conference on Communications (ICC), pp.6774-6779, June 2012.

[27] K.Dimou, M.Wang, Y.Yang, M.Kazmi, A.Larmo, J.Pettersson, W.Muller, "Handover within 3GPP LTE: Design principles and performance", in Proc. IEEE Veh. Technol. Conf.(VTC Fall), pp.1-5, Sep.2009.

[28] H.S.Park, H.S.Yoon, T.H.Kim, J.S.Park, M.S.Duo, J.Y.Lee, "Vertical handover procedure and algorithm between IEEE 802.11 WLAN and CDMA cellular network, Mobile Communications", pp.103-112, 2003.

[29] C.Lima, M.Bennis, and M.Latva-aho, "Modeling and analysis of handover failure probability in small cell networks", in Computer Communications Workshops, IEEE Conference pp.736-741 April 2014.

[30] Q.Liao, S.Stanczak, and F.Penna, "A statistical algorithm for multi objective handover optimization under uncertainties", in Proc. IEEE Wireless Commun. Netw. Conf. (WCNC), pp.1552-1557, April 2013.

[31] K.Vasudeva, M.Simsek, and I.Guvenc, "Analysis of handover failures in Hetnets with layer-3 filtering", in Wireless Communications and Networking Conference (WCNC), 2014 IEEE, pp.2647-2652, April 2014.

[32] C.de.Lima, M.Bennis, and M.Latva-aho, "Modeling and analysis of handover failure probability in small cell networks", in Computer Communications Workshops (INFOCOM WKSHPS), 2014 IEEE Conference on, April 2014, pp.736-741.

[33] X.Lin, R.Ganti, P.Fleming, and J.Andrews, "Towards understanding the fundamentals of mobility in cellular networks", Wireless Communications, IEEE Transactions on, vol.12, no.4, pp.1686-1698, April 2013.

[34] K.Kitagawa, T.Komine, T.Yamamoto, and S.Konishi, "A handover optimization algorithm with mobility robustness for LTE systems", in IEEE 22nd International Symposium on Personal Indoor and Mobile Radio Communications, Sept.2011, pp.1647-1651.

[35] Y.Lee, B.Shin, J.Lim, and D.Hong, "Effects of time-to-trigger parameter on handover performance in SON-based LTE systems", in 16^{th} Asia-Pacific Conference on Communications, Oct.2010, pp.492-496.

[36] K.Kitagawa, T.Komine, T.Yamamoto, and S.Konishi, "Performance evaluation of handover in LTE-advanced systems with pico cell range expansion, in IEEE 23rd International Symposium on Personal Indoor and Mobile Radio Communications, Sept.2012, pp.1071-1076.

[37] B.Jeong, S.Shin, I.Jang, N.W.Sung, and H.Yoon, "A smart handover decision algorithm using location prediction for hierarchical macro/femto cell networks", in Vehicular Technology Conference (VTC Fall), 2011 IEEE, Sept.2011, pp.1-5.

[38] S.Barbera, P.Michaelsen, M.Saily and K.Pedersen, "Improved mobility performance in lte co-channel Hetnets through speed differentiated enhancements", in IEEE Globecom Workshops, Dec. 2012, pp.426-430.

[39] I.Guvenc, "Capacity and fairness analysis of heterogeneous networks with range expansion and interference coordination", IEEE Communications Letters, vol.15, no.10, pp.1084-1087, Oct.2011.

[40] N.Zia, S.Mwanje, and A.Mitschele-Thiel, "A policy based conflict resolution mechanism form lb and mro in LTE self-optimizing networks, in Computers and Communication (ISCC), 2014 IEEE Symposium on, June 2014, pp.1-6.

[41] B.Zhang, W.Qi, and J.Zhang, (2017), "A Markov Based Performance Analysis of Handover and Load Balancing in HetNets", Int.J.Communications, Network and System Sciences, 10, pp.223-233.

[42] Nikolaos D.Tselikas, 18th International Conference on Transparent Optical Networks (ICTON), 2016.

[43] Q.Shen, J.Liu, Z.Huang, X.Gan, Z.Zhang, and D.Chen, "Adaptive double thresholds handover mechanism in small cell LTE-A network, in Wireless Communications and Signal Processing (WCSP), 2014 Sixth International Conference on, Oct.2014, pp.1-6.

[44] C.Prehofer, N.Nafisi, Q.Wei, "A Framework for Context-aware Handover Decisions, in 14^{th} IEEE 2003 International Symposium on Personal Indoor and Mobile Radio Communication Proceedings, Sept. 2003 pp.7-10

[45] Q.Wei, K.Farkas, C.Prehofer, P.Mendes ,"Context-aware Handover Using Active Network Technology.

[46] Yi.Zhang, M.Wu, Shu.Ge, Li.Luan, An.Zhang, "Optimization of Time-to-Trigger Parameter on Handover Performance in LTE High-speed Railway Networks, in Proc IEEE 2012 pp.251-255

[47] T.S.Rappaport, Wireless Communications: Principles& Practice, 2nd ed. Englewood Cliffs, NJ, USA: Prentice-Hall, 2002.

[48] 3GPP (2013) TR 36.842: Study on Small Cell Enhancements for E-UTRA and E-UTRAN; Higher Layer Aspects, Rel-12.

[49] A. Goldsmith, Wireless Communications. Cambridge, U.K.: Cambridge Univ. Press, 2005.